D3.7

Data acquisition analytic tools for IMS & GMS

Project No	GA824160
Project Acronym	EnTimeMent
Project full title	ENtrainment & synchronization at multiple TIME scales in the MENTal foundations of expressive gesture
Instrument	FET Proactive
Type of action	RIA
Start Date of project	1 January 2019
Duration	48 months

Distribution level	[PU][1]
Due date of deliverable	Month 30
Actual submission date	July 2021
Deliverable number	3.7
Deliverable title	Data acquisition analytic tools for IMS & GMS.
Type	
Status & version	
Number of pages	21
WP contributing to the deliverable	3
WP / Task responsible	EuroMov
Other contributors	ALL
Author(s)	EuroMov, IIT_GE, IIT_FE, UNIGE, UCL
EC Project Officer	Christiane WILZECK
Keywords	Computational models, Software libraries, Movement analysis and prediction, Machine learning; Motion Capture

Abbreviations

EU	European Union
EC	European Commission
PU	Public
WP	Work Package

Table of Contents

1. Introduction

This deliverable reports on the progress on the research conducted between M1-M30 of the EnTimeMent project with regards to the Individual Motor Signature (IMS) and Group Motor Signature (GMS) during complex and joint action execution and observation.

This deliverable is strongly connected, also in organisation (numbering) of the content, to deliverable D3.1 (Phase 1), deliverable D3.5 (Joint Action), D3.6 (Complex Action), which is about the hardware and software tools used for acquiring and analysing data in the context of single, joint and complex actions. As such, this document focuses only on the tools of sub-projects specific for definition of IMS and GMS and the Emotion Motor Signature (EMS) and contains references to other deliverables reporting on the D1.7 Models and Algorithms; D2.2; Results on prediction in action execution and observation – Phase 2, and Research Requirements D1.2).

A plethora of research suggests that emotional and idiosyncratic content is best conveyed by the distal parts of the body (which bare relatively low energy expense cost for moving) during gross motor acts with a high number of degrees of freedom. Thus, plethora of research suggests that a specific relation exists between motion, individual characteristics and dimensions of emotion, which we explore in combination with multiple timescales approach as a part of EnTimeMent project.

2. Data Acquisition Tools

This section describes the software (processing pipelines), sensors, and other devices used for capturing data in four main settings of the EnTimeMent project: controlled lab settings, unconstrained lab settings, musical performance settings, and everyday (e.g., home) settings.

Please note that the numbering of the subsections refers to numbering used for experimental work in D1.2 Research Requirements, to maintain continuity throughout the project deliverables.

2.1.4 IMS in pointing task (IIT – FE)

The abundance of degrees of freedom available during AE suggests that different joint configurations, as well as spatio-temporal patterns of muscle activity, can equally be used to reach the same behavioral goal (Bernstein 1967). Although a handful of kinematic solutions are biomechanically valid, everyday actions (i.e. reaching for an object on the floor starting from a standing posture) are usually performed via a limited number of possible kinematic configurations of the biomechanical chain (e.g. “ankle” and “hip” strategies for postural control; Horak and Nashner 1986; Berret et al. 2009). On the top of that, each individual carry his own robust and yet unique way of moving (Individual Motor Signature – IMS; Hilt et al. 2016; Słowiński et al. 2016). For instance, in a whole-body reaching task Hilt and collaborators (Hilt et al. 2016) showed low intra-subject motor variability, accompanied by a large inter-subject variability.

We asked naive participants to perform a whole-body reaching action which could be executed with numerous IMSs generally spread within a continuum between two “extreme” patterns (ankle and knee strategies; Hilt et al. 2016).

Task

The action execution task was replicated from a previous study (Hilt et al. 2016) investigating the different motor strategies when pointing towards a homogeneous

surface and without a specific target. This protocol was chosen because it keeps free the subjects from external constraints (e.g. a precise point to reach) and evokes natural inter-subject variability. Participants were asked to perform a series of whole-body pointing movements towards a uniform opaque curtain fixed to a wooden frame (2.5 tall × 1.5 m large; see Fig. 1) positioned at a 15° angle with respect to the vertical. The surface was a black curtain (tissue) mounted on a wooden frame, soft enough to prevent subjects from using it as a support when finishing the movement but sufficiently elastic to keep its shape and remain flat. Subjects were told that they could point at any position they wanted over the surface. Starting from a standing position and at a distance of 130% of arm's length from the surface, subjects had to move all body parts with the only constraint to keep the feet fixed and to move both arms simultaneously. The request to move the two arms together ensured that all markers lay approximately along the para-sagittal plane (Berret et al. 2009) to limit the kinematic analysis to this plane (right hemibody in 2D coordinates). All subjects were able perform the task. Ten trials were run before and after the action observation protocol. More importantly, this protocol by avoiding external constraints (e.g., a precise target to reach), allows subjects to execute the movement they would naturally/spontaneously use (e.g., IMS). A previous study using this task observed a large movement variability across subjects but low intra-subject variability (Hilt et al. 2016). Interestingly, subjects behaviors were a trade-off between the optimization of two distinct cost functions. The first strategy (named Ankle) limits mechanical energy expenditure but uses a kinematic configuration that may be risky for equilibrium maintenance: bending the body forward using mainly ankle and shoulder joints while freezing knee and hip joints (large center of pressure forward displacement). In muscular terms, the ankle strategy is associated with a pre-activation of the tibialis anterior (anticipatory postural adjustment) followed by an inhibition of this muscle later in the movement. The second strategy (named Knee) increases mechanical energy expenditure but uses a kinematic configuration that may be safer for equilibrium maintenance: substantial knee flexion and forward trunk bending associated with a backward hip displacement (limited center of pressure forward displacement). In muscular terms, the knee strategy implied an activation of lower-leg muscles (including tibialis anterior) during the movement.

Kinematic recordings

Whole-body movements in 3 axes (mediolateral, X; anteroposterior, Y; vertical, Z) were recorded using a seven cameras motion capture system (Vicon, Oxford, UK) sampling at 100 Hz. Eight retro-reflective markers (15 mm in diameter) were recorded. Markers were placed at the following anatomical locations on the right side of the body: the acromial process (named here “shoulder”), the lateral condyle of the humerus (named here “elbow”), the styloid process of the ulnar (named here “wrist”), the last phalanx of the index finger (named here “index”), the greater trochanter (named here “hip”), the knee interstitial joint space (named here “knee”), the ankle external malleolus (named here “ankle”) and the fifth metatarsal head of the foot (named here “toe”).

Angular computation

We first defined five segments: foot (from toe to ankle), shank (from ankle to knee), thigh (from knee to hip), trunk (from hip to shoulder) and arm (from shoulder to elbow). We computed then the elevation angle (angle with the gravity’s vertical) of each segment in the sagittal plane via the following equation:

$$\theta_{segAB} = tan^{-1}\left(\frac{B_y - A_y}{B_z - A_z}\right) \quad \text{(Eq.1)}$$

Where θ_{segAB} represents the elevation angle of the segment linking *A* to *B* having for cartesian coordinates in the sagittal plane (A_y, A_z) and (B_y, B_z) respectively.

Elevation angle are constrained by the anatomical limit of each joint, and never reach values higher (or lower) than 2π (or -2π respectively). In 2D, knowing these constraints, intersegmental angles can be deduced directly from elevation angles. The intersegmental angle between the two segments Seg_A and Seg_B is equal to the subtraction of the elevation angle of Seg_B to the elevation angle of Seg_A. Elevation and resulting intersegmental angles are illustrated in supplementary figure 2 left and right panel respectively.

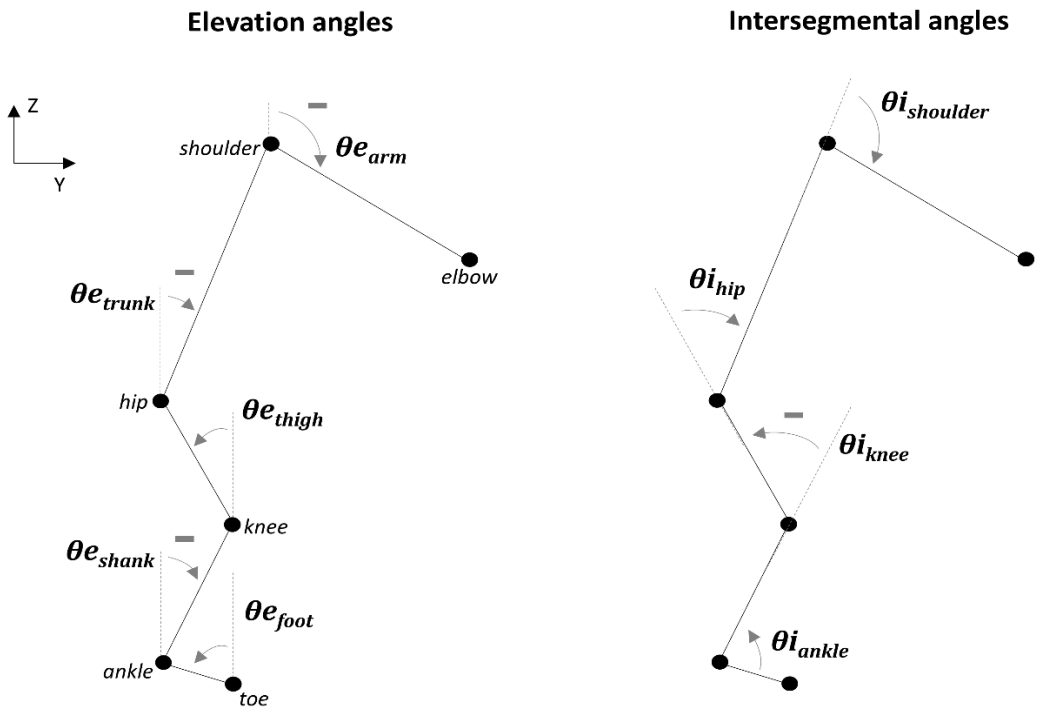

Figure 1: Illustration of the computed elevation angles (left panel) and intersegmental angles (right panel) in the (Y,Z) plane. Angles are represented by a grey arrow. The sign "**-**" above an arrow indicates that the angle for this final posture is negative. Kinematic markers are represented by black dots.

IMS index

We computed an individual action execution index (IMS index) by normalizing (z-score) and averaging the final value of the four intersegmental angles considered. Considering that each joint angle has different maximal amplitude (e.g. ankle versus hip), the z-score normalization ensures that the final index (average of all angles) is not reflecting the contribution of only the joint having the largest range of motion. This index is a simple way to represent the final kinematic configuration of each subject and may thus be considered as description of the postural strategy implemented by each participant.

IMS distances

To complement the IMS index, we evaluated the difference/similarity between the IMS of each subject and the actor's implementation of the two IMSs. To this aim, we defined a distance by computing the root mean squared error (RMSE) between inter-

segmental angular trajectories of the actor and each of the subjects. RMSE is commonly used to compute the average magnitude of the errors between experimental values and associated model predictions (Hilt et al. 2016).

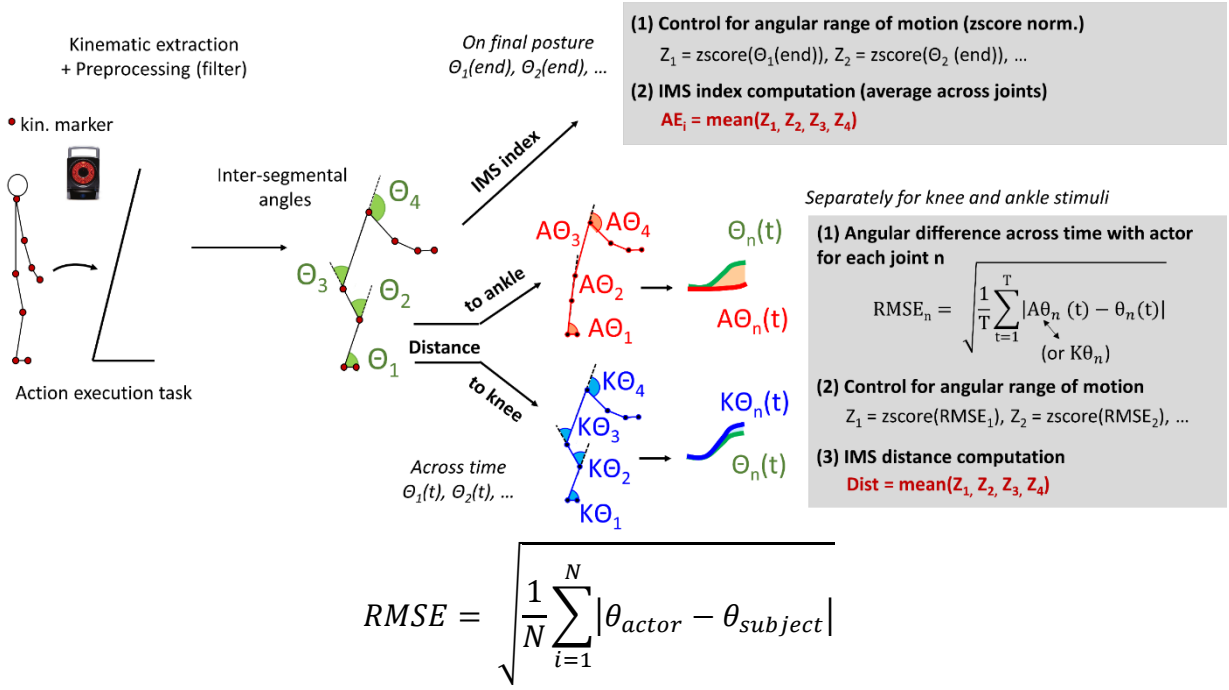

$$RMSE = \sqrt{\frac{1}{N}\sum_{i=1}^{N}\left|\theta_{actor} - \theta_{subject}\right|}$$

All trials were time-normalized (from t_{start} to t_{end}) to 100 frames. For each subject and each joint (ankle, knee, hip, and shoulder) we computed an averaged angular trajectory that we compared (using RMSE) with the corresponding angular trajectory of the actor in both IMSs. RMSE were then normalized across subjects (z-score) and averaged across joints, to obtain a unique distance value for each pairwise comparison between subject's and actor's IMSs. From this point, $Dist_{ankle}$ and $Dist_{knee}$ will refer to the distance between the IMSs of subjects and the video-stimuli respectively showing the ankle strategy and the knee strategy.

Computing in this way, the distances are taking into account the whole duration of the movement while the IMS index refers to only the final posture (see Figure 2). There's obviously some degree of overlapping variance between the two, but they are built using different data, potentially describing very different processes. The first one addressing the dynamic component of reaching the final posture, while the other describing the final posture only.

Figure 2: Illustration of the different steps to compute the AE index (upper part) and AE distances (lower part) to ankle IMS (red) and knee IMS (blue).

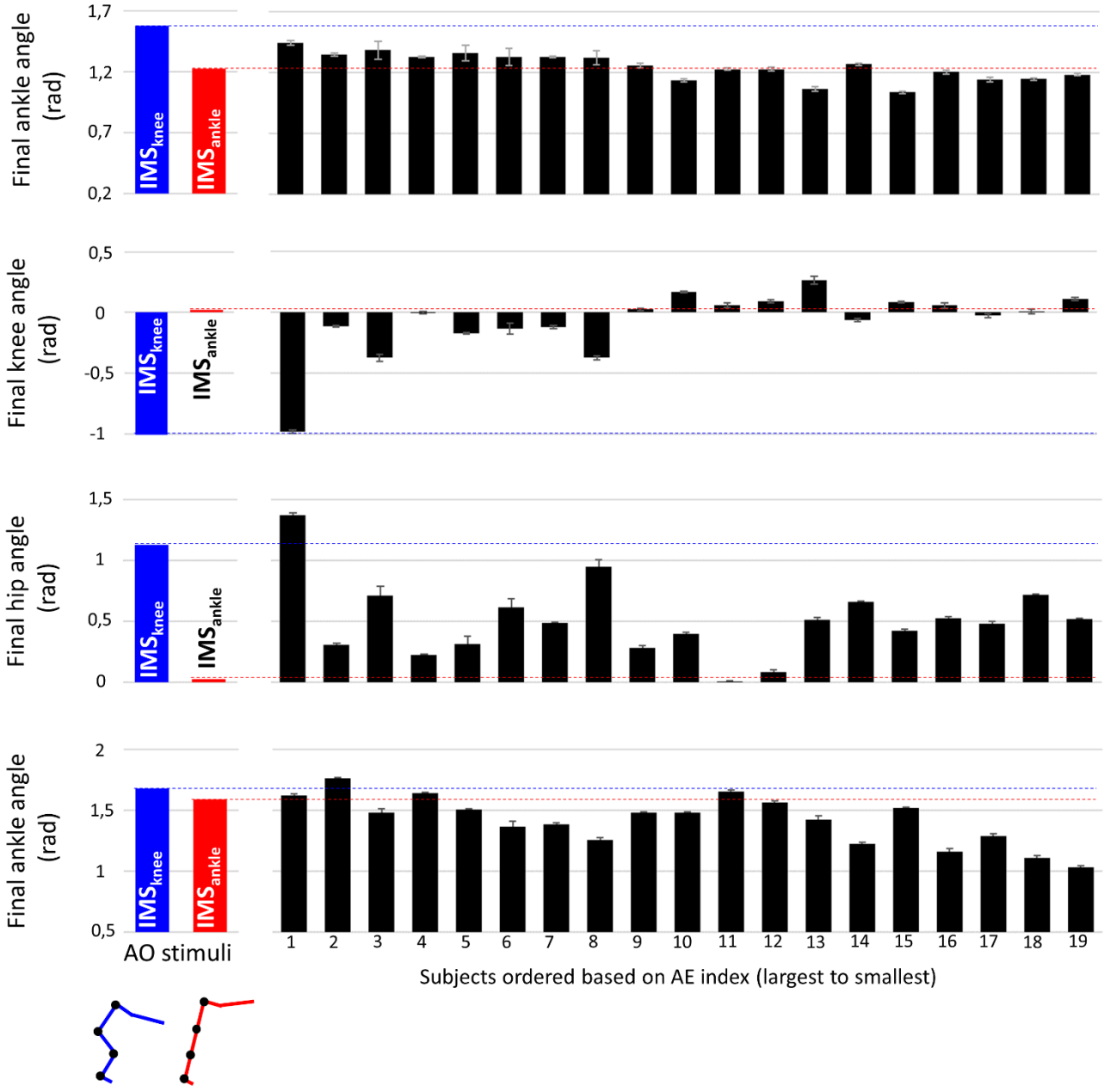

Figure 3. Final intersegmental angular values for each subject (1 to 19; ordered from the largest to the smaller AE index) and each joint (ankle, knee, hip, shoulder), averaged across AE trials (pre and post AO). For each subject, standard error encompasses the variability across trials and session (pre and post AO). As a reference, we added the corresponding value for each stimulus (IMS_{knee}, IMS_{ankle}). No standard error can be computed for stimuli because they refer to one video (i.e., trial) of the actor. These graphs illustrate the expected large difference between subjects IMS and the small intra-subject variability (relatively small standard error).

Table 1. Mean and standard error (across subjects) of the final intersegmental angles of the ankle, knee, hip and shoulder, extracted from the kinematics recorded in the action execution task pre-AO (left column), post-AO (right column). The third column presents the results of the permutation test comparing the values pre-AO and post-AO of each intersegmental angle.

Mean ±ste (rad)	pre-AO	post-AO	Statistic
Ankle	1.26 ±0.03	1.25 ±0.03	p=0.69, t=0.41
Knee	-0.09 ±0.08	-0.09 ±0.07	p=0.99, t=0.01
Hip	0.51 ±0.08	0.50 ±0.07	p=0.91, t=0.12
Shoulder	1.43 ±0.05	1.41 ±0.05	p=0.40, t=0.88

References

Bernstein NA. 1967. The Coordination and Regulation of Movements. Pergamon P. ed. Oxford.

Berret B, Bonnetblanc F, Papaxanthis C, Pozzo T. 2009. Modular Control of Pointing beyond Arm ' s Length. J Neurosci. 29:191–205.

Hilt PM, Berret B, Papaxanthis C, Stapley P, Pozzo T. 2016. Evidence for subjective values guiding posture and movement coordination in a free-endpoint whole-body reaching task. Sci Rep. 6:23868.

Horak FB, Nashner LM. 1986. Central programming of postural movements: adaptation to altered support-surface configurations. J Neurophysiol. 55:1369–1381.

Slowiński P, Alderisio F, Zhai C, Shen Y, Tino P, Bortolon C, Capdevielle D, Cohen L, Khoramshahi M, Billard A, Salesse R, Gueugnon M, Marin L, Bardy BG, di Bernardo M, Raffard S, Tsaneva-Atanasova K. 2017. Unravelling socio-motor biomarkers in schizophrenia. npj Schizophr. 3.

2.1.14 Automatic Detection in the Context of Movement with Chronic Pain based on Novel Multiple-Timescales Machine Learning Architectures (UCL)

Please see (for more information on the method):

Wang et al. 2021 https://dl.acm.org/doi/abs/10.1145/3463508

We explored a GC-LSTM neural network, shown in **Error! Reference source not found.**, which is based on GC [Kipf and Welling 2017] and LSTM [Hochreiter and Schmidhuber 1997; Gers et al. 1999] neural networks. Each GC network (GCN) takes in the joints positions at time *t* in motion capture data from time *t*=1 to time *t*=*T* where *T* is the duration of the movement sequence in frames. Specifically, the graph *G* of the network is defined as $\mathrm{G} = \{N, E\}$ such that

$$n = \left[x_{t_n}^i, y_{t_n}^i, z_{t_n}^i (, \alpha^i)\right]$$

where $n \in N$, $x_{t_n}^i, y_{t_n}^i, y_{t_n}^i$=3D joint position, and α^i=contextual data (e.g. activity), and edges are defined with the adjacency matrix

$$A \in \{0, 1\}^{N \times N}$$

i.e., 1 (edge exists) where there is a direct link between two joints in the data and 0 (no edge) otherwise. The outputs of the GCN for each time *t* are concatenated and fed into the LSTM neural network (LSTMNN) and the outputs of the LSTMNN are in turn fed into module of full-connected layers (i.e., a multilayer perceptron) which classifies its input based on the label of interest. The results of our exploration of the GC-LSTM network for automatic detection of multiple movement characteristics (protective behaviour and activity) is given in deliverable D2.2. A discussion of the rationale behind these experiments is provided in D1.7.

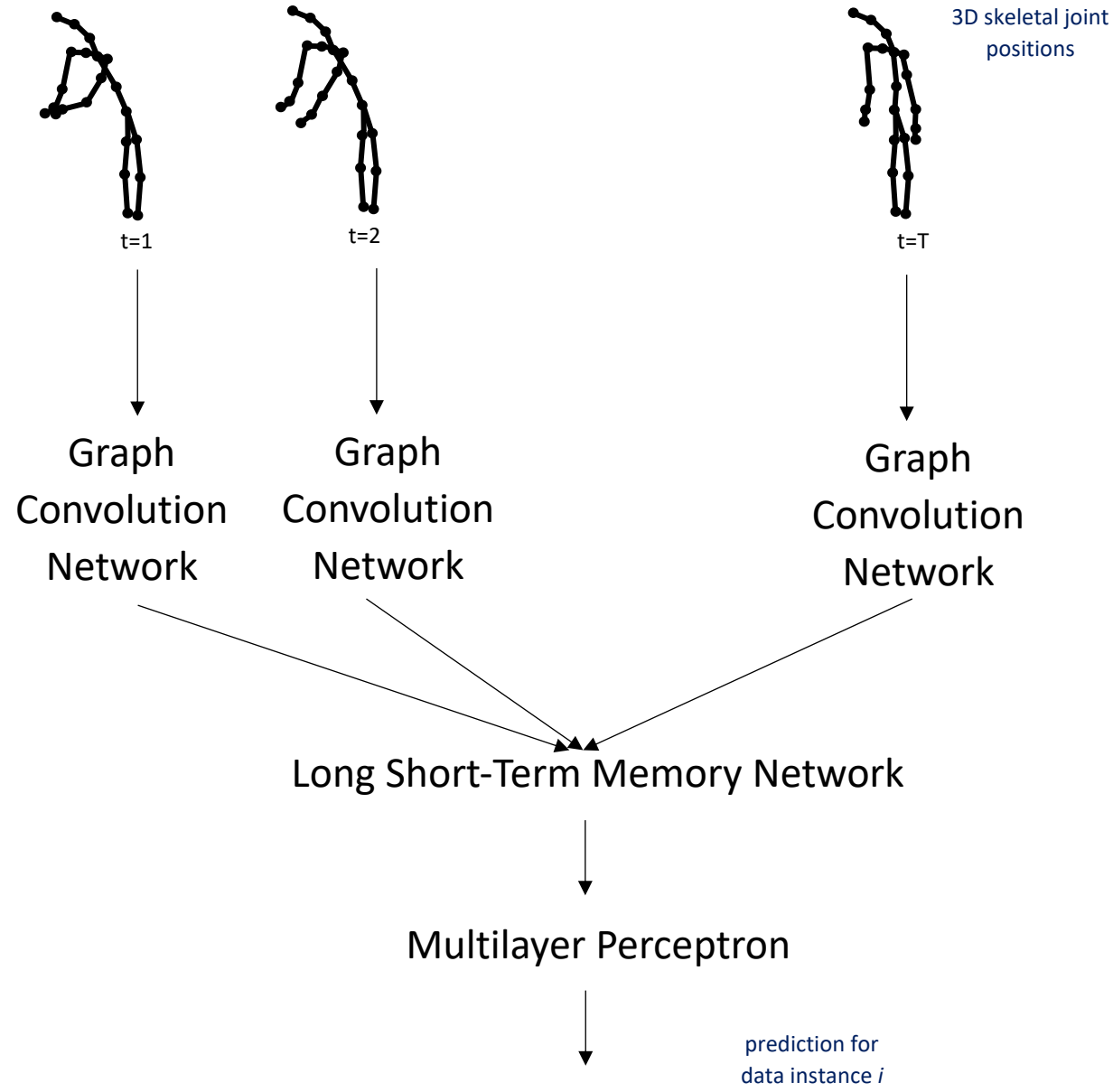

Figure 1. Graphical Convolution and Long Short-Term Memory (GC-LSTM) Neural Network

References

Wang, C., Williams, A., Lane, N., and Bianchi-Berthouze, N. (2021). "Leveraging Activity Recognition to Enable Protective Behavior Detection in Continuous Data." Proceedings of the ACM on Interactive, Mobile, Wearable and Ubiquitous Technologies 5 (2): 1–24.

Kipf, T., and Welling, M. (2017). Semi-supervised classification with graph convolutional networks. In 5th International Conference on Learning Representations (ICLR).

Hochreiter, S. and Schmidhuber, J. (1997). Long Short-Term Memory.Neural Comput.9, 8 (Nov. 1997), 1735–1780. https://doi.org/10.1162/neco.1997.9.8.1735.

Gers, F., Schmidhuber, J. and Cummins, F. (1999). Learning to forget: continual prediction with LSTM. In1999 Ninth International Conference on Artificial NeuralNetworks ICANN 99. (Conf. Publ. No. 470), Vol. 2. 850–855 vol.2. https://doi.org/10.1049/cp:19991218.

2.2.6 DuoMotion: EMS (EuroMov)

Please see:
Lozano-Goupil J, Bardy BG and Marin L (2021) Toward an Emotional Individual Motor Signature. Front. Psychol. 12:647704.
https://www.frontiersin.org/articles/10.3389/fpsyg.2021.647704/full

2.3.3 Time to sync: Emosync (EuroMov)

Individual Motor Signatures (IMS) refers to the the idiosyncratic way each individual moves (e.g., Słowiński et al. (2016)). Pioneering work of Johansson (1973) put forward the notion of transformational invariants (Malcolm, 1953), i.e., that persistence in some dimensions (e.g., length, ratios) across the motion of others (e.g., global transformation of the local optic flow) could help observers to quickly extract person-related properties, very relevant to socio-motor interaction context. IMS often relies on movement velocity as a key feature, as it is both stable across time and repetitions for each individual (movement similarity) and differential between individuals (inter-individual movement difference). Differences in the way people move during the performance of a motor task can be captured by using 95% confidence interval ellipses in the similarity space (Słowiński et al., 2016). This is an abstract two-dimensional geometrical space minimizing distances between repetitions and individuals by using ad-hoc dimensional reduction techniques. Ellipses can be large or small depending on intra-individual variability and can be close or distant from each other depending on between-individual variability. The approach has proven useful in identifying IMS in various populations, ranging from healthy individuals to people suffering from schizophrenia (e.g., Słowiński et al. (2017)). It has also proven useful in various tasks and contexts such as in the mirror game (Słowiński et al., 2016) or during improvisation movement (e.g., Coste et al. (2019)), and at different distal or proximal

(and more postural) parts of the body (e.g., Coste et al. (2021)). Whether IMS, {as well as Group Motion Signatures (GMS, inter-group movement differences), i.e., the way IMS are assembled together in an ensemble of individuals engaged in reaching a common goal during joint action}, are emotionally neutral, and whether they are of different shapes and locations in the similarity space when produced in various emotional contexts (intra-subject variability) remains open to investigation (see Lozano-Goupil et al. (2021), for a first evaluation of Emotional IMS).

The Emosync experiment investigated the human multi-modal social synchronisation occurring at different time scales, and looked into emergence of GMS during the joint action performance. The participants were performing a collective dancing improvisation task. Specifically, the task was to create complex, interesting and variable movements with their right hand alone and while standing in the group. The impact of social context as well as embodied emotions are investigated within the expressive gesture. Below we present tools used respectively for a heart rate and movement analysis in the context of IMS and GMS.

Heart Rate analysis

Apparatus

The Trigno EKG Biofeedback Sensor (Delsys) was used to record the cardiac activity with the resolution of 2148 Hz. The software for acquisition was EMGworks version 4.7.3.0. Electrodes were placed in accordance with Delsys guidelines by using the modified 3-lead EKG setup under the pectoral muscles to diminish possible noise from muscle activation.

Pre-processing, Filtering and Event detection

The raw ECG data were preprocessed before the analysis and filtered from exogeneous effect. The chosen method was the sym4 wavelet due to its similarity with the QRS complex (Mallat, & Peyré, 2009). Firstly, the raw data were identified with the wavelet method and most of the files was correctly identified (Figure 1). The upper graph represents the RR-interval (sec) between two successive heartbeats.

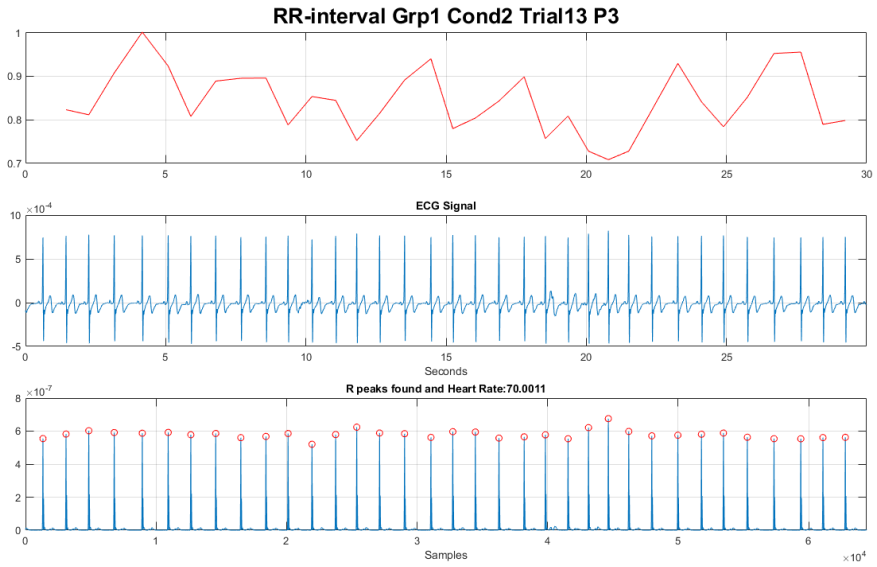

Figure 1. Example of a correct detection

Then, the physiologically impossible values due to specificity of the task lower than 30 bpm and higher than 180 were cut. Afterwards, the files were visually examined to detect problematic trials that needed adjustments with respect to the choice of parameters (Figure 2).

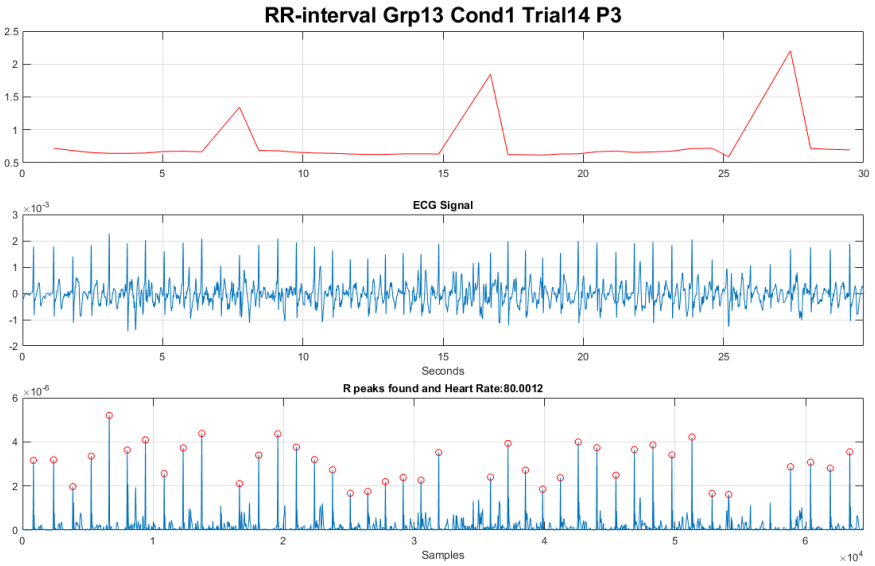

Figure 2. Example of a poor detection.

Overall, there were 79 problematic trials out of 1287 ECG trials in total. Next, the adjustments were performed manually with respect to the height of the peak and distance between two successive peaks (Figure 3). The improved detection was achieved by manual adjustment.

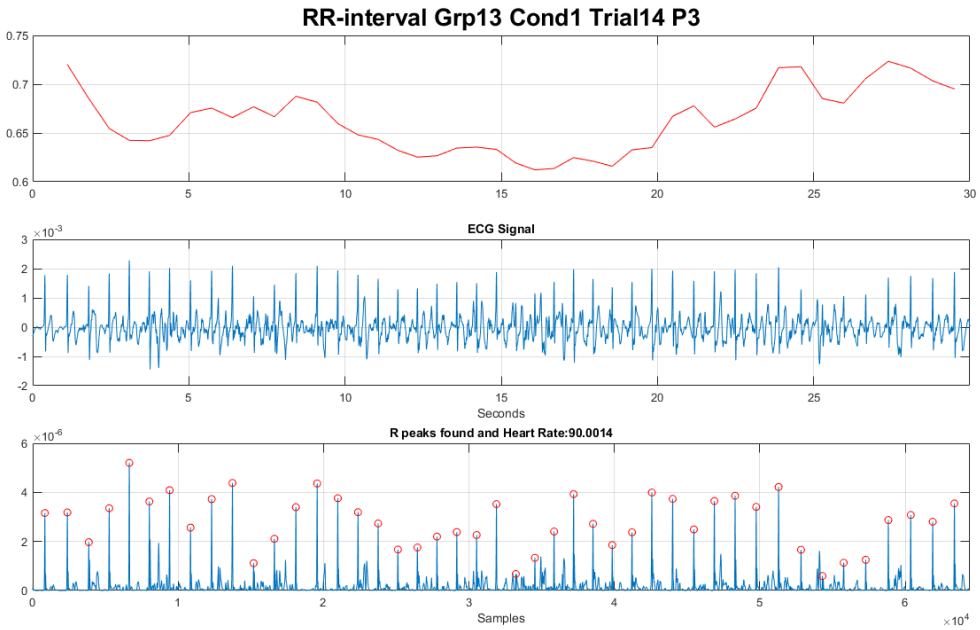

Figure 3. Example of an improved detection

Recurrence quantification analysis to compute synchronization

No interpolation was performed during the preprocessing stage for performing the recurrence quantification analysis (RQA) because the interpolation has an important the exogeneous influence on the RQA metrics. The recurrence quantification analysis and its modification help to quantify the synchronisation between the time series presenting nonlinear characteristics (Romano et al., 2005). Parameters are selected for each individual time series (embedding dimensions and delay), reconstruction into phase space, selection of radius radius of the phase space where the behaviour / signal which enters this radius is considered reoccurrence, generation of reoccurrence plot and then proceed to calculation of metrics (such as DET, RR and MaxL). Below is the visualization (Figure 4) of raw data, spline interpolation 4Hz and spline interpolation of 20 Hz. As a result, the metric of determinism DET, which identifies the patterned sequence of behavior, increased from .62 performed on the raw data to .97 and 1 to spline interpolations of 4hz and 25 Hz respectively).

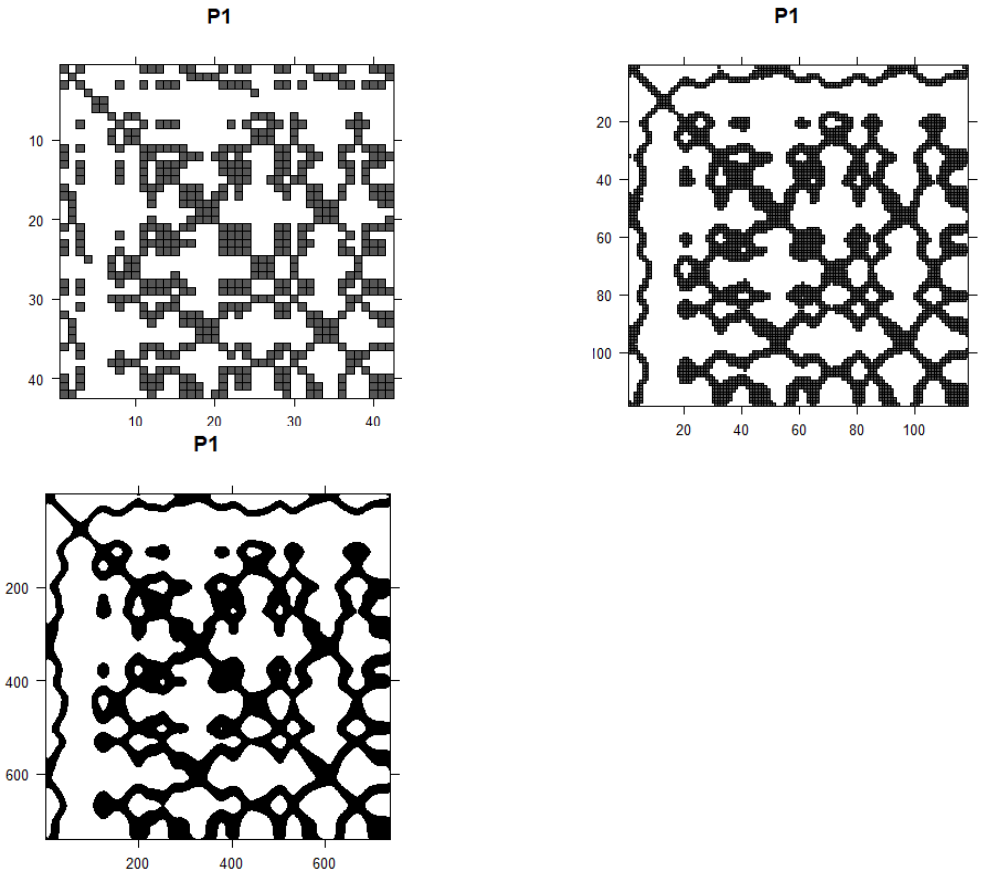

Figure 4. Example of reoccurrence plots.

Movement Analysis – Identification of IMS/GMS

Movement data was captured with Vicon Motion Capture technology and analyzed with Nexus software. Each participant had markers placed on the base of the index fingers, wrist, forearm and headband. The index finger markers were used to quantify the interactional synchrony between the participants as well as the motor signatures. For IMS identification and the further GMS derivation we base on the results of Słowiński and collaborators (2016). Specifically, the probability distribution functions of the performed movement velocities and then transformed them to cumulative distributions functions. Next, the difference between the velocities was calculated via the Earth Mover's distance method. Finally, these differences were projected onto the abstract geometrical space for visualization. Each point within the graph represents one trial performed by one person. The number next to the point indicates which of the 3 participants performed the trial. All of the trials represented by individual points are englobed within ellipse. Within the Emosync experiment, the participants performed

Solo and Group conditions. Overall, there are two ellipses to visualize differences between Solo and Group conditions and they are denoted with S and G respectively. Finally, next to the letter representing the condition, there is a number indicating negative (i.e., -1), neutral (i.e., 0), and positive (i.e., 1) emotions (Figure 5).

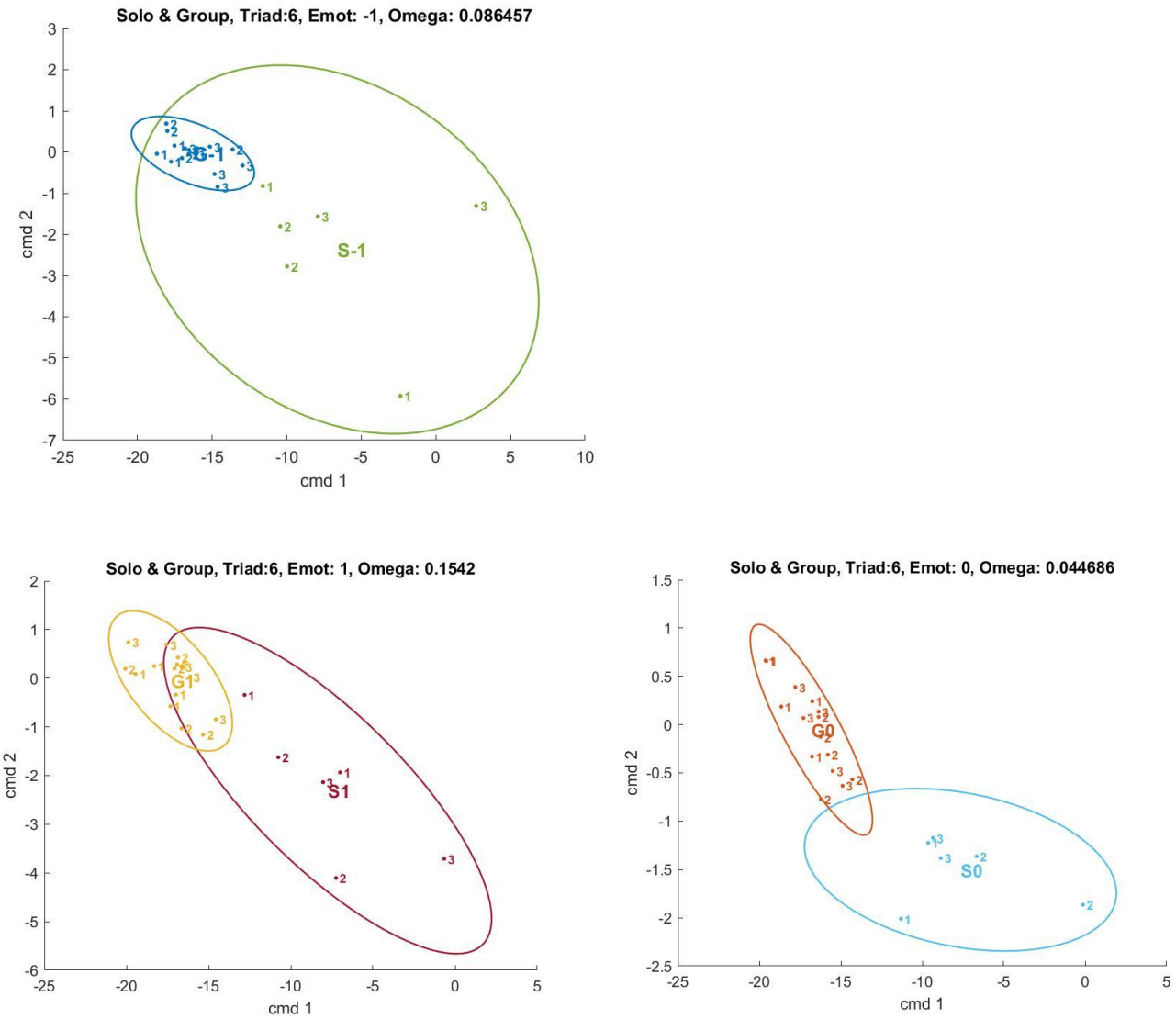

Figure 5. Visualization of differences the IMS and GMS for different emotions.

We then build upon the Słowiński's et al. (2016) relative position errors to the calculation within 3 dimensions. Particularly, they calculated relative position error to identify the entrainment within the interaction:

$$(x1(t) - x2(t))sgn(v1(t))$$

However, these measures were designed for laboratory setting of 1D oscillations and they are not applicable within the 3D coordinate system, where the real movement occurs. That is why we've adapted this formula to 3D coordinate system (Table 1):

$$(v1(t) - v2(t))sgn(a1(t))$$

Table 1. Relative Velocity Error

Triad	Positive	Neutral	Negative
1	0.75	0.77	0.62
2	0.60	0.58	0.55
3	0.61	0.61	0.48
4	0.78	0.45	0.51
5	0.77	0.57	0.81
6	0.15	0.04	0.09
7	0.59	0.45	0.37
8	0.64	0.71	0.61
9	0.62	0.67	0.29
10	0.19	0.37	0.38
11	0.63	0.56	0.39
12	0.58	0.66	0.69
13	0.50	0.39	0.40

References

Coste, A., Bardy, B.G., Marin, L., 2019. Towards an Embodied Signature of Improvisation Skills. Front. Psychol. 10, 2441. https://doi.org/10.3389/fpsyg.2019.02441

Coste, A., Bardy, B.G., Janaqi, S., Słowiński, P., Tsaneva-Atanasova, K., Goupil, J.L., Marin, L., 2021. Decoding identity from motion: how motor similarities colour our perception of self and others. Psychol. Res. 85, 509–519. https://doi.org/10.1007/s00426-020-01290-8

Coste, A., Bardy, B.G., Marin, L., 2019. Towards an Embodied Signature of Improvisation Skills. Front. Psychol. 10, 2441. https://doi.org/10.3389/fpsyg.2019.02441

Mallat, S. G., & Peyré, G. (2009). *A wavelet tour of signal processing: The sparse way* (3rd ed. / Stéphane Mallat with contributions from Gabriel Peyré, Vol. 54). Amsterdam, London: Academic Press.

Romano, M. C., Thiel, M., Kurths, J., Kiss, I. Z., & Hudson, J. L. (2005). Detection of synchronization for non-phase-coherent and non-stationary data. *Europhysics Letters (EPL)*, *71*(3), 466–472. https://doi.org/10.1209/epl/i2005-10095-1

Słowiński, P., Zhai, C., Alderisio, F., Salesse, R., Gueugnon, M., Marin, L., . . . Tsaneva-Atanasova, K. (2016). Dynamic similarity promotes interpersonal coordination in joint action. *Journal of the Royal Society, Interface*, *13*(116). https://doi.org/10.1098/rsif.2015.1093

Słowiński, P., Alderisio, F., Zhai, C., Shen, Y., Tino, P., Bortolon, C., Capdevielle, D., Cohen, L., Khoramshahi, M., Billard, A., Salesse, R., Gueugnon, M., Marin, L., Bardy, B.G., Di Bernardo, M., Raffard, S., Tsaneva-Atanasova, K., 2017. Unravelling socio-motor biomarkers in schizophrenia. npj Schizophr. 3. https://doi.org/10.1038/s41537-016-0009-x